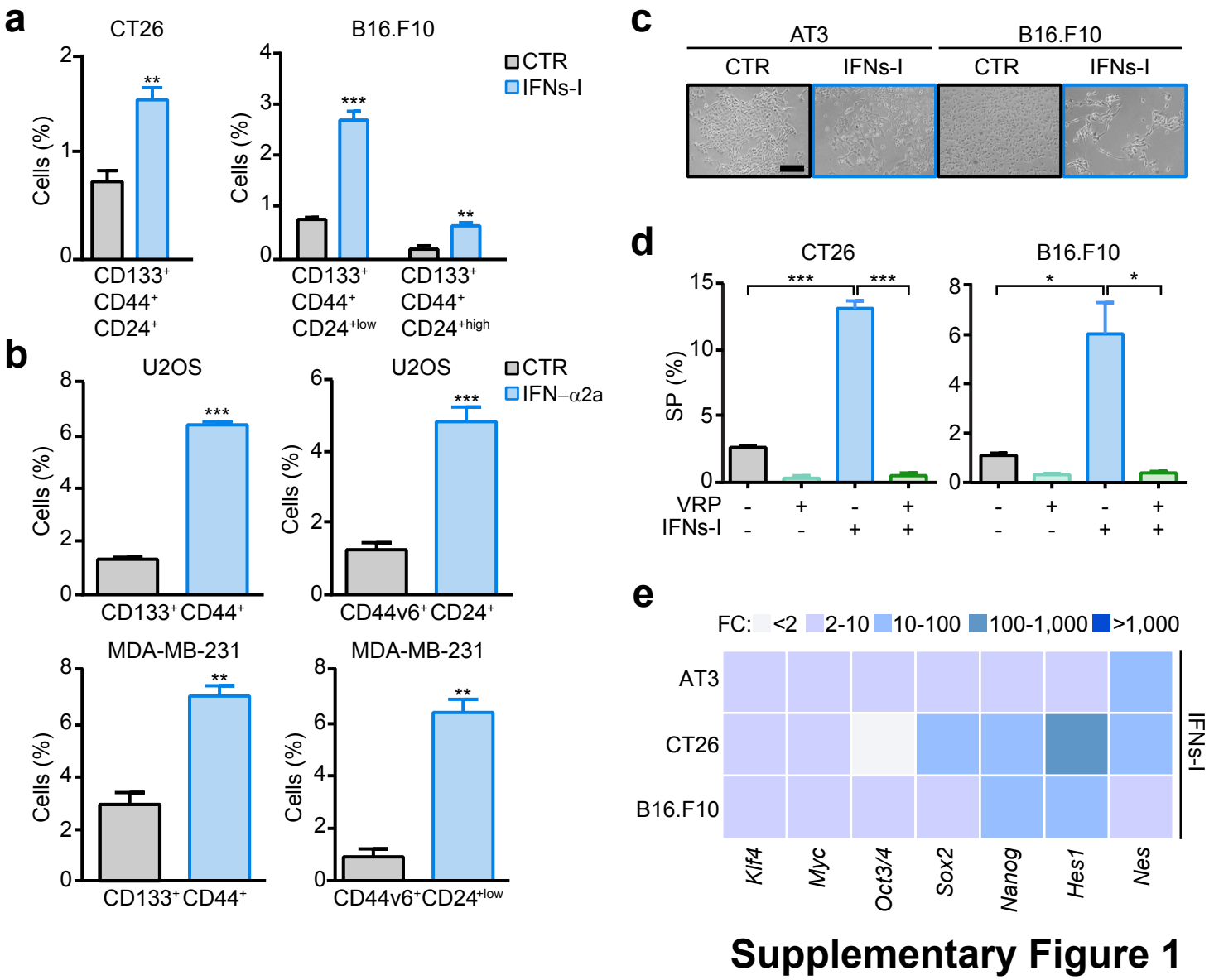

Supplementary Figure 1

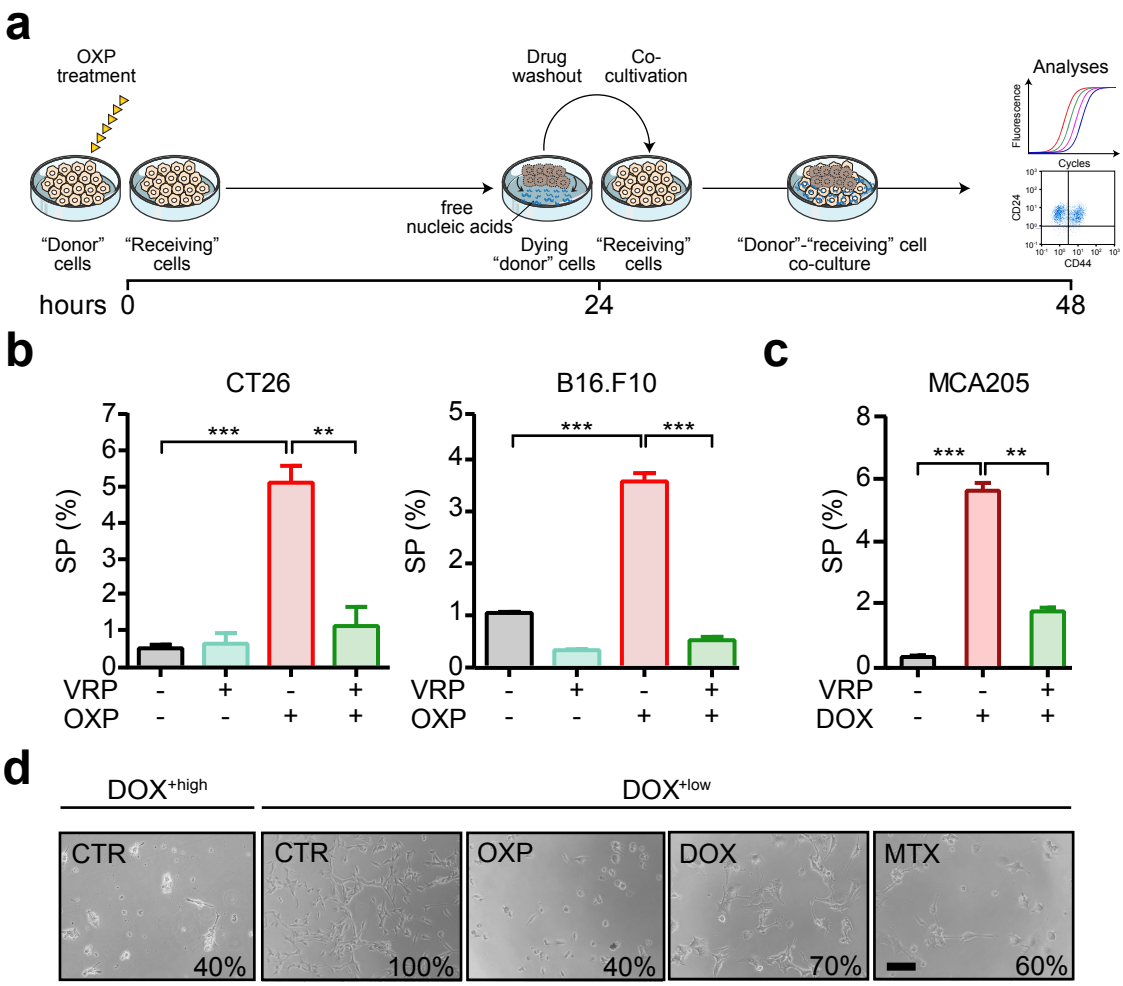

Supplementary Figure 2

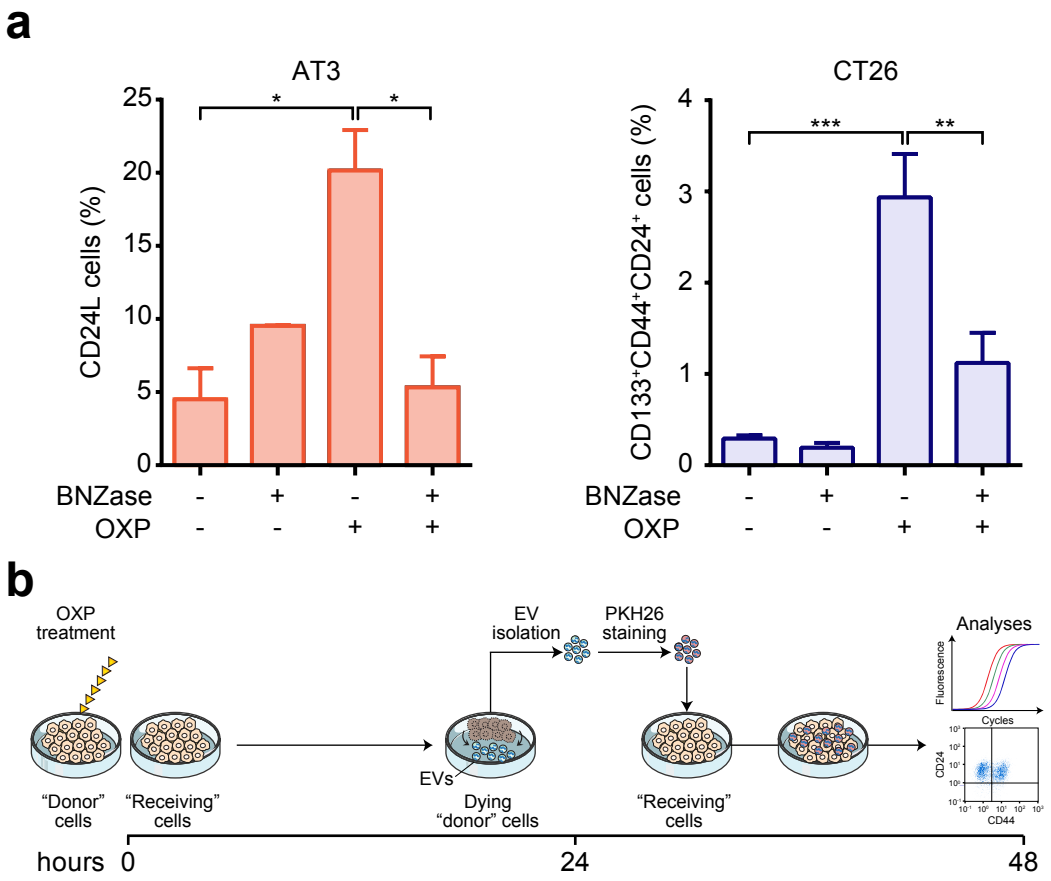

Supplementary Figure 3

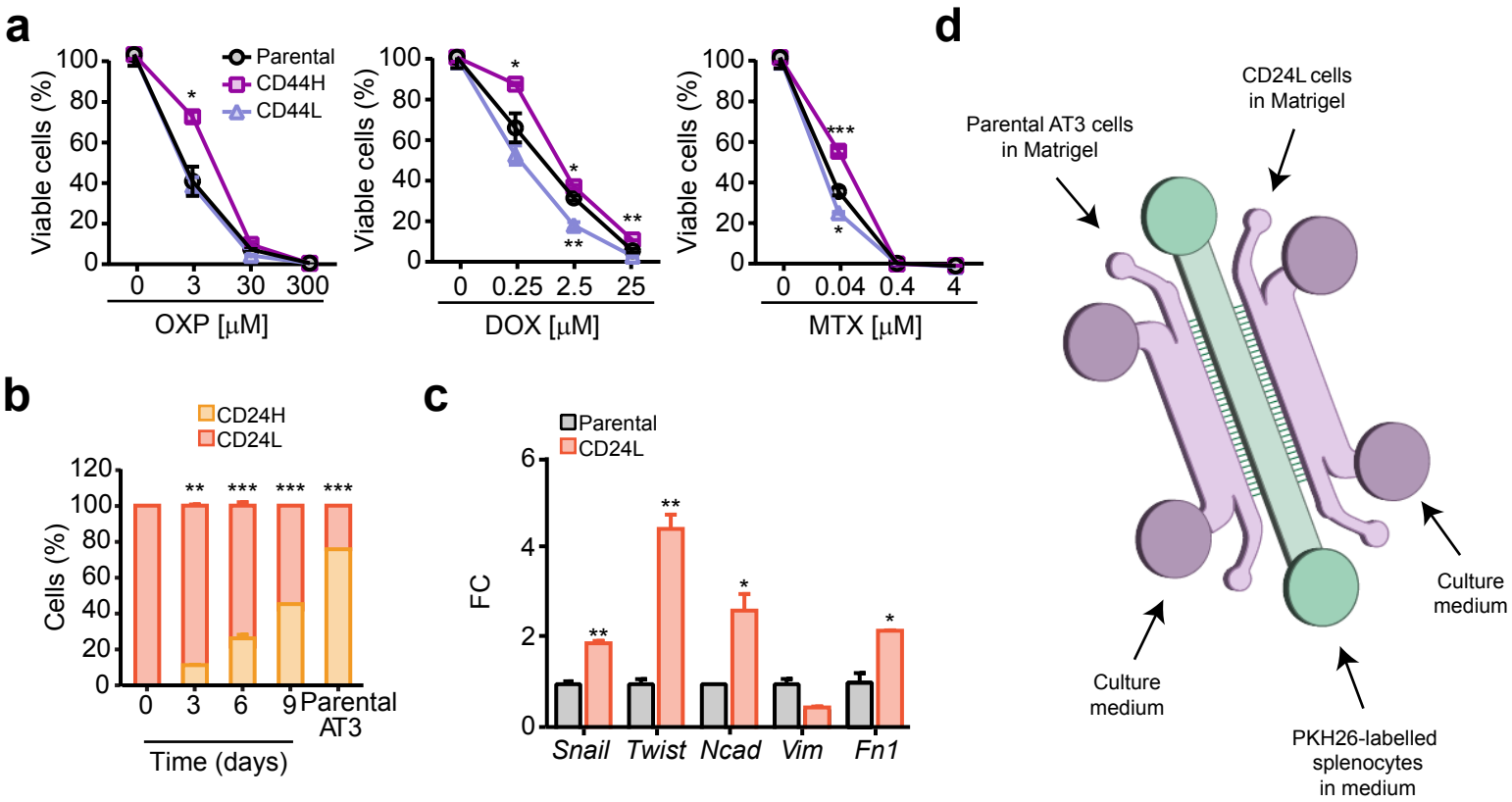

Supplementary Figure 4

a

cell growth arrest
Kifc1,Cdk1,Ptgs2,Bub1,Bub1b,Cenpe,Ccnb1,Prr11,Aurka,Cdkn3,Plk1,Fhl1,Sema3a,Cth,Grem1,Sema3g
GO:0045786, GO:0030308

cell differentiation
Ptgs2,Kif14,Ccnb1,Ereg,Aurka,Grem1,Cdc20,Sema3a,Fam83d,Snai2,Sema3g
GO:0021700, GO:0048762

oxidative phosphorylation
Cdk1,Ccnb1
GO:1903862

protein dephosphorylation
Dusp5,Prkar2b,Errfi1,Plk1,Ptpn22,Psph,Inpp4b,Cdca2,Dusp5,Cdc25c,Cdkn3,Ptpn22
GO:0033673, GO:0016311

Type-I-IFN signaling
Oas3,Cd74,Oasl2,Bst2,Parp10,Irf7,Oas2,Irgm2,Zbp1,Rtp4,Trim12a,Bcl2l11,Dtx3l,Parp9,Ddx58
GO:0050792, GO:0009615

Type-II-IFN signaling
Gbp9,Irgm2,Gbp3,Parp14,Gbp7,Irgm1,Bst2,Parp9
GO:0034341

immune suppression
Gpnmb,Cd74,Grn,Nr1d1,Parp3
GO:0002695

APC machinery
H2-Q4,Tap1,Tapbp,H2-K1,H2-D1
GO:0019885

lipid metabolism
Irs1,Cpt1a,Cd74,Vdr,Wdr81,Slc27a1,C3/Nr1d1
GO:0019216

autophagic cell death
Bmf,Cd74,Trp53inp1,Mmp9,Bcl2l11,Steap3,Fgfr1,Hsph1,Irgm2,Trim12a,Trp53inp1,Wdr81,Irgm1,Trp53inp2,Dcn,Map1lc3b
GO:2001233, GO:0006914

cell growth
Irs1,Sox9,Fgfr1
GO:0010464

cell stemness
Sox9,Klf10,Sox4
GO:0035019

tissue remodeling
Gpnmb,Vdr,Mmp9,Sema3c,Tpp1,P2rx7,Mmp2
GO:0048771

DNA damage response (stress response)
Dtx3l,Steap3,Parp9,Parp3
GO:2001022

chromatin binding
Dtx3l,Parp9
GO:0035563

b

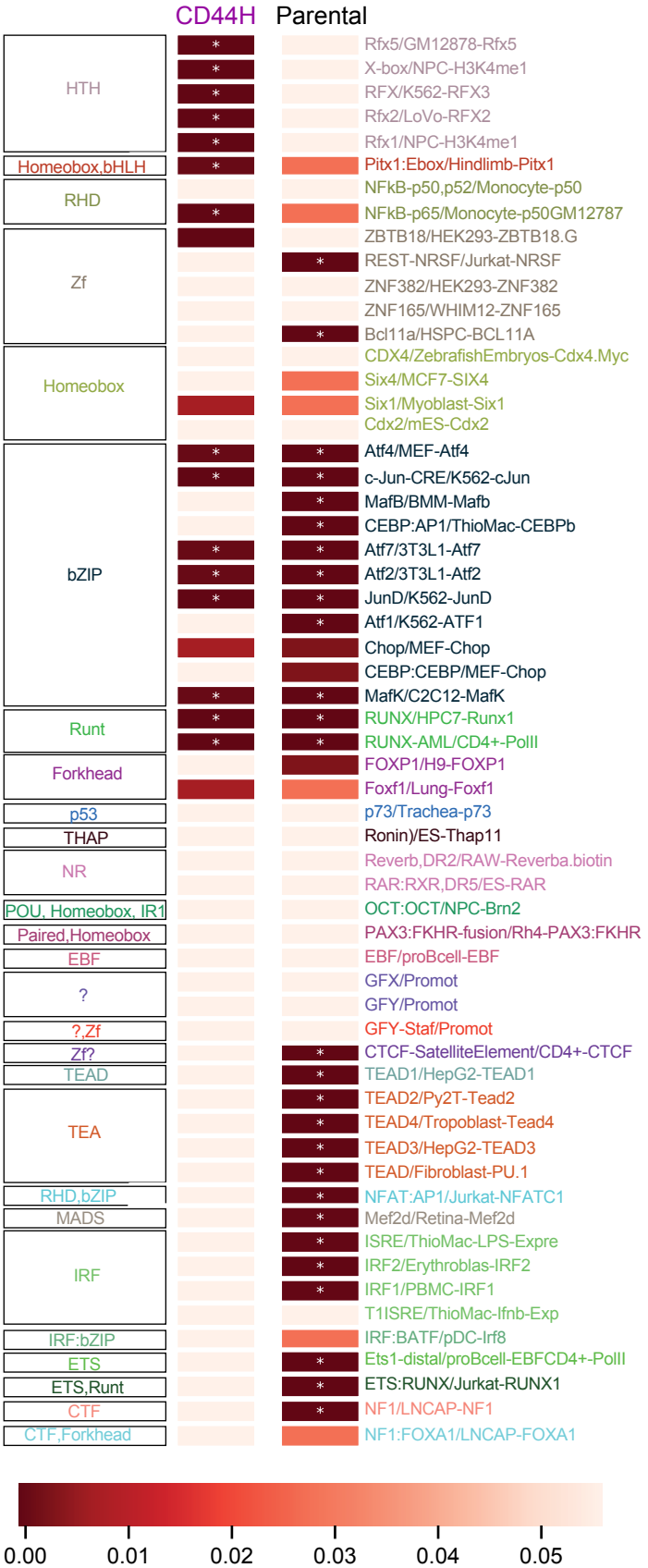

Supplementary Figure 5

Supplementary Table 1. Patient characteristics.

Parameter	Value (*n* = 20)
Age	
Median range	53.5 (30-77)
Sex	
Female	20 (100%)
Male	0 (0%)
Histological type	
Invasive ductal carcinoma	19 (95%)
Ductal carcinoma *in situ*	0 (0%)
Invasive lobular carcinoma	1 (5%)
Histological grade at diagnosis	
II	6 (30%)
II/III	6 (30%)
III	7 (35%)
Unknown	1 (5%)
ER* *status* at diagnosis	
Positive	15 (75%)
Negative	5 (25%)
Unknown	0 (0%)
PR *status* at diagnosis**	
Positive	13 (65%)
Negative	7 (35%)
Unknown	0 (0%)
HER2* *status* at diagnosis**	
Positive	16 (80%)
Negative	4 (20%)
Unknown	0 (0%)
Ki-67 *status* at diagnosis	
Positive	19 (95%)
Negative	0 (0%)
Unknown	1 (5%)
Number of chemotherapy cycles	
4	1 (5%)
5	1 (5%)
7	1 (5%)
8	14 (70%)
10	1 (5%)
Unknown	2 (10%)
Histological grade at surgery	
II	4 (20%)
II/III	0 (0%)
III	13 (65%)
Unknown	3 (15%)
ER *status* at surgery	
Positive	14 (70%)
Negative	6 (30%)
Unknown	0 (0%)
PR *status* at surgery	
Positive	10 (50%)
Negative	10 (50%)
Unknown	0 (0%)
HER2 *status* at surgery	
Positive	13 (65%)
Negative	7 (35%)
Unknown	0 (0%)
Ki-67 *status* at surgery	
Positive	19 (95%)
Negative	0 (0%)
Unknown	1 (5%)

Abbreviations: *ER, estrogen receptor; **PR, progesterone receptor; ***HER2, human epidermal growth factor receptor 2.

SUPPLEMENTARY FIGURE LEGENDS

Supplementary Figure 1. IFN-I-mediated enrichment of CSCs. (**a,b**) Multiparametric flow cytometry analysis of the CSC surface markers CD133, CD44 and CD24 in CT26 colon carcinoma and B16.F10 melanoma murine cell lines (**a**) and U2OS osteosarcoma and MDA-MB-231 breast carcinoma human cell lines (**b**). Cells were treated with mock (CTR) or purified IFNs-I (murine cell lines) or recombinant IFN-α2a (human cell lines) (6000 U/mL, 72h). The percentage (mean±SEM; $n \geq 3$) of $CD133^{+}CD44^{+}CD24^{+}$ CT26 cells, $CD133^{+}CD44^{+}CD24^{+low}$ and $CD133^{+}CD44^{+}CD24^{+high}$ B16.F10 cells, $CD133^{+}CD44^{+}$ and $CD44v6^{+}CD24^{+}$ U2OS cells, and $CD133^{+}CD44^{+}$ and $CD44v6^{+}CD24^{+low}$ MDA-MB-231 cells is shown. (**c**) Microscopic analysis of AT3 breast carcinoma and B16.F10 murine cell lines treated with mock (CTR) or purified IFNs-I (6000 U/mL, 72h). Representative pictures of AT3 and B16.F10 epithelial cell morphology under IFN-I treatment. The scale bar indicates 100 μm. (**d**) Flow cytometry analysis showing the proportion of SP (Hoechst 33342^{-} SP within PI^{-}) cells in CT26 and B16.F10 cell lines left untreated (black) or treated with (VRP, 100 μM, light green), or purified IFNs-I (6000 U/mL 72h, blue) or VRP+IFNs-I (dark green). Data are presented as mean±SEM of one representative experiment out of two. (**e**) Expression levels of reprogramming factors in AT3 breast carcinoma, CT26 colon carcinoma and B16.F10 melanoma murine cell lines treated with purified IFNs-I (6000 U/mL, 72h). Data are reported as mean FC±SEM (n=2) over untreated cells after intrasample normalization to the levels of *Ppia*. *P<0.05, **P<0.01, ***P<0.001 (**a,b**) unpaired t test with Welch's correction, (**d**) ordinary one-way ANOVA test followed by Bonferroni's correction. CSC, cancer stem cell; CTR, control; FC, fold change; IFNs-I, Type I interferons; PI, propidium iodide; SP, side population; VRP, verapamil.

Supplementary Figure 2. Immunogenic chemotherapy triggers putative CSC appearance. (**a**) Schematic representation of the "donor"–"receiving" cell co-culture experimental protocol. (**b,c**) Flow cytometry analysis showing the proportion of SP (Hoechst 33342^{-} within PI^{-}) cells in CT26

colon carcinoma, B16.F10 melanoma (**b**) and in MCA205 sarcoma (**c**) murine cells left untreated or treated with OXP (30 μM) (**b**) or DOX (2.5 μM) (**c**) alone or in combination with VRP (100 μM) for 48h. Data are presented as mean±SEM of at least two independent experiments. (**d**) Representative pictures of FACS-isolated DOX^{+low} and DOX^{+high} cells in standard culture conditions and under treatment with different chemotherapeutic agents (DOX^{+low} cells). MCA205 cells were firstly treated with 2.5 μM DOX for 48h, and then FACS-isolated based on their low or high positivity for red fluorescence. DOX^{+low} and DOX^{+high} sorted cells were then left untreated (CTR) or treated with OXP (30 μM), DOX (2.5 μM) or MTX (0.04 μM) for 48h. Representative pictures of CTR DOX^{+high} cells and CTR and treated DOX^{+low} are shown. The percentage of counted cells is indicated for each condition, as determined by cell counts on pictures by using ImageJ software. $^{**}P<0.01$, $^{***}P<0.001$ (**b**,**c**) ordinary one-way ANOVA test followed by Bonferroni's correction. CSC, cancer stem cell; CTR, control; DOX, doxorubicin; FACS, fluorescence activated cell sorting; MTX, mitoxantrone; OXP, oxaliplatin; PI, propidium iodide; SP, side population; VRP, verapamil.

Supplementary Figure 3. CSC enrichment through nucleic acid transfer. (**a**) Flow cytometry analysis of CSC surface markers in "receiving" viable AT3 breast carcinoma and CT26 colon murine carcinoma cells upon co-culturing with "donor" cells of the same type previously treated with OXP (300 μM, 48h) alone or in combination with BNZase (200 IU/mL, 48h). Data are presented as mean±SEM ($n\geq2$ for AT3 and $n\geq3$ for CT26). (**b**) Schematic representation of the EV-"receiving" cell co-culture experimental protocol. $^{***}P<0.001$ (**a**) one-way ANOVA test followed by Bonferroni's correction. BNZase, benzonase; CSC, cancer stem cell; EV, extracellular vesicles; OXP, oxaliplatin.

Supplementary Figure 4. Characterization of IFN-I-enriched CSCs. (**a**) Evaluation of cell proliferation/viability by CellTiter-Glo® assay in parental and FACS-isolated CD44H and CD44L IFN-CSC MCA205 subsets treated with OXP, DOX or MTX (72h) as indicated. Results are

reported as means±SEM of one representative experiment out of three. (**b**) Flow cytometry analysis of the regenerative potential of CD24L and CD24H AT3 cells isolated by FACS upon enrichment by OXP (300 μM, 48h) treatment, maintained in standard culture conditions and analyzed by flow cytometry upon co-staining with antibodies directed against CD133, CD44, and CD24 at the indicated time points. (**c**) qRT-PCR analysis of the expression level of cell-invasion molecules in parental and CD24L AT3 cells (isolated as in **b**). Data are reported as mean FC±SEM over untreated cells after intrasample normalization to the expression levels of the housekeeping gene *Ppia* (*n*=2). (**d**) Schematic representation of "competition" microfluidic devices. **P*<0.05, ***P*<0.01, ****P*<0.001 (**a**) one-way ANOVA test followed by Bonferroni's correction, (**b**) ordinary two-way ANOVA test followed by Bonferroni's correction, (**c**) unpaired *t* test with Welch's correction. CD24H, $CD133^{+}CD44^{+}CD24^{+high}$; CD24L, $CD133^{+}CD44^{+}CD24^{+low}$; CD44H, $CD133^{+}CD24^{+}CD44^{+high}$; CD44L, $CD133^{+}CD24^{+}CD44^{+low}$; CSC, cancer stem cell; DOX, doxorubicin; FACS, fluorescence activated cell sorting; FC, fold change; IFNs-I, Type I interferons; IFN-CSCs, Type I interferon-induced CSCs; MTX, mitoxantrone; OXP, oxaliplatin.

Supplementary Figure 5. Chromatin remodeling following IFN-I exposure. A list of selected genes upregulated (red) and downregulated (blue) in CD44H IFN-CSCs and used to generate a GO network analysis (*see* **Figure 6e**) is reported in **a**, while TF motifs enriched at least 2-fold for each locus as identified by ATAC-seq are shown in **b**. * adjusted $P \leq 0.001$. ATAC-seq, assay for transposase-accessible chromatin using sequencing; CD44H, $CD133^{+}CD24^{+}CD44^{+high}$; GO, gene ontology; IFNs-I, Type I interferons; IFN-CSCs, Type I interferon-induced CSCs; TF, transcription factor.

Supplementary Figure 6. Clinical correlation between *KDM1B*, IFN-I signature, stemness and immune evasion in BC patients. (**a**) Spearman correlations between IFN-I-related, stem-related and immune regulatory-related gene expression scores from microarray data of three publicly available cohorts of patients with BC treated with neo-adjuvant anthracycline-based chemotherapy.

*P<0.05, **P<0.01, ***P<0.001. (**b,d,e**) BC patient stratification based on risk behaviour via the Metabric platform (https://ega-archive.org/) and expression of low (blue) or high (orange) levels of *SOX2* (GenBank/Entrez ID: 6657) and either *KDM1B* (GenBank/Entrez ID: 221656), or *MX1* (GenBank/Entrez ID: 4599), or *CXCL10* (GenBank/Entrez ID: 3627), or *OASL* (GenBank/Entrez ID: 8638). (**c**) Kaplan-Meier plots depicting LRFI in BC patients according to risk behavior (*P* Cox, Log-Rank Mentel-Cox *P* value was calculated using the Metabric website). BC, breast cancer; IFN-I, Type I interferon; LRFI; local relapse-free incidence.

Supplementary Movie 1. This movie shows the interaction of splenocytes from C57Bl/6J mice with parental AT3 breast carcinoma murine cells. Cells were loaded into microfluidic devices and monitored by fluorescence videomicroscopy for 72h. Microphotographs were taken every 2min for a total of 720 frames/day. Two x 10^6 mouse splenocytes and 5 x 10^4 tumor cells were loaded into the chambers at the bottom right and bottom left of the channels (outside the camera view), respectively. As splenocytes were attracted, they progressively appeared in the camera plan.

Supplementary Movie 2. This movie shows the interaction of splenocytes from C57Bl/6J mice with CD24L AT3 ICD-CSCs. Cells were loaded into microfluidic devices and monitored by fluorescence videomicroscopy for 72h. Microphotographs were taken every 2min for a total of 720 frames/day. Two x 10^6 mouse splenocytes and 5 x 10^4 tumor cells were loaded into the chambers at the bottom right and bottom left of the channels (outside the camera view), respectively. As splenocytes were weakly attracted, only few cells appeared in the camera plan. Note that CSCs are non-adherent cells, thus they are mostly out of focus. CD24L, $CD133^+CD44^+CD24^{+low}$; ICD-CSCs, immunogenic cell death-induced CSCs.

Supplementary Movie 3. Time-lapse recording detail showing the strong, persistent and productive interaction of mouse splenocytes with parental AT3 breast carcinoma murine cancer cells (cropped from **Supplementary Movie 1**).

Supplementary Movie 4. Time-lapse recording detail showing the weak, rapid and inefficient interaction of mouse splenocytes with CD24L AT3 ICD-CSCs (cropped from **Supplementary Movie 2**). CD24L, $CD133^{+}CD44^{+}CD24^{+low}$; ICD-CSCs, immunogenic cell death-induced CSCs.

Supplementary Table 1. Patient characteristics.